Journal of Biomolecular Structure & Dynamics, ISSN 0739-1102
Volume 29, Issue Number 3, (2011)

Lose Weight with Traditional Chinese Medicine? Potential Suppression of Fat Mass and Obesity-Associated Protein

http://www.jbsdonline.com

Pei-Chun Chang[a#]
Jing-Doo Wang[a#]
Min-Min Lee[a#]
Su-Sen Chang[b]
Tsung-Ying Tsai[b]
Kai-Wei Chang[b]
Fuu-Jen Tsai[a,b]
Calvin Yu-Chian Chen[a,b,c,d,e*]

[a]Department of Bioinformatics, Asia University, Taichung, 41354, Taiwan
[b]Laboratory of Computational and Systems Biology, School of Chinese Medicine, China Medical University, Taichung, 40402, Taiwan
[c]China Medical University Beigang Hospital, Yunlin, Taiwan
[d]Department of Systems Biology, Harvard Medical School, Boston, MA 02115, USA
[e]Computational and Systems Biology, Massachusetts Institute of Technology, Cambridge, MA 02139, USA.
[#]Equal Contribution.

[*]Phone: +886-4-2205-3366
E-mail: ycc@mail.cmu.edu.tw; ycc929@MIT.EDU (C.Y.-C. Chen)

Abstract

Overweight and obesity are common health problems in modern society, particularly in developed countries. Excessive body mass has been linked to numerous diseases, such as cardiovascular diseases, diabetes, and cancer. Fat mass and obesity-associated protein (FTO) activity have direct impact on food intake and results in obesity. Inhibition of FTO activity may cause weight loss and reduce obese-linked health risks. We investigated the potential weight loss effects of traditional Chinese medicine (TCM), particularly by inhibiting FTO functions. Molecular docking was performed to screen TCM compounds from TCM Database@Taiwan (http://tcm.cmu.edu.tw). Three candidates were identified that contained either a tetrahydropyridine group or potent electronegative phenol group in the structure scaffold. Molecular dynamics simulation analysis of the docking poses of each complex indicated stabilizing trends in the protein-ligand complex movements. In addition, the number of hydrogen bonds increased throughout the 20 ns simulation. These results suggest that these TCM candidates could be potential FTO inhibitors through competitive inhibition.

Key words: Obesity; Traditional Chinese Medicine (TCM); FTO; Docking; Molecular Dynamics.

Introduction

The fat mass and obesity-associated protein (FTO), as the name suggests, has been linked to human obesity (1, 2). In mice models, the regulation of blood glucose metabolism in liver by FTO further implied relationships between FTO and obesity (3, 4). Genome-wide association studies and mouse models further determined *FTO* gene as one of the critical genes that could induce obesity (3-6). FTO is also involved in obesity related diseases, such as cardiovascular diseases (7, 8), hypertension (9), polycystic ovary syndrome (10), and type II diabetes (11). Recent studies further suggest that *FTO* gene may be linked to Alzheimer's disease (12), breast cancer (13), susceptibility to cognitive degradation (14, 15), and infertility (16).

FTO is a member of the AlkB family of 2-oxoglutarate-dependent oxidative DNA/RNA demethylases. This protein is associated with demethylation of 3-methylthymine in single-stranded DNA (17) and is associated with food intake (18, 19) and pre-adeposite differentiation (5, 20). Overexpression of *FTO* has been reported to affect fat metabolism and cause obesity (21). Scientific evidence strongly supports the relationship between FTO and obesity (22-24).

According to the 2011 World Health Organization's (WHO) statistical report based on statistics collected in 2008, over 1.5 billion adults over the age of 20 are

considered overweight, in which 200 million men and nearly 300 million women are obese (25). Moreover, nearly 43 million children under the age of five were overweight in 2010 (25). Obesity has been reported to induce cardiovascular disease, diabetes, and cancer (4, 26). In 2008, over $147 billion US dollars were spent in resolving obesity-related diseases (12). Considering FTO is closely associated with obesity, regulation of FTO expression is consequently a potential target in fighting this disease (27, 28).

This study aimed to identify potential FTO inhibitors or its precursors from traditional Chinese medicine (TCM). TCM is a common traditional medical practice among East Asia. Compared to synthetic drugs, the medical contents of TCM could be easily extracted and analyzed. In addition, existing TCM documents provide relevant information for the medical uses of a perspective drug. Current studies have further identified many potential TCM applications, such as anti-cancer (29), anti-inflammation (30), and cardiotonic effects (30). However, few scientific analysis of TCM treatment against obesity was reported. This study focused on identifying TCM compounds that inhibit lipid uptake through FTO pathways. *In silico* pharmacology methods have been adopted for high throughput compound analysis in modern drug development (31-43) and was employed in this study. The compatibility between FTO and over 20,000 TCM compounds from TCM Database@Taiwan (http://tcm.cmu.edu.tw) (44) was assessed using structure-based virtual screening algorithm. The identified potential compounds were subjected to molecular dynamics (MD) simulation to determine their respective binding stabilities within FTO.

Materials and Methods

Virtual Screening

Over 20,000 3D small TCM molecules were collected from TCM Database@Taiwan (44). Duplicate compounds were discarded and the remaining compounds were subjected to Lipinski's Rule of Five (45) to identify drug-like candidates. The resulting 7,500 TCM compounds were adjusted to physiological settings using the Prepare Ligand module in Discovery Studio 2.5 (DS 2.5; Accelrys Inc., San Diego, CA) and virtually screened against the FTO crystalized protein structure from RCSB Protein Data Bank (PDB ID: 3LFM) (46). The docking site was defined by the 3-methylthymidine from the same FTO structure data. CHARMm force field (47) was applied to the FTO prior to docking. Docking algorithm was performed using DS 2.5 LigandFit module (48). Multiple dock scores of each docking pose were calculated.

Molecular Dynamics Simulation

MD simulation was performed for the candidate docking poses using the Dynamic Cascade protocol from DS 2.5. Each input complex was minimized by Steepest Descent (500 steps) in fixed conformation, followed by 500 Conjugate Gradient steps in flexible conformation. Each complex was then heated for 50 ps from 50 K to 310 K and equilibrated for 200 ps. The MD trajectory of each complex was monitored for 20 ns under fixed temperature (NVT canonical ensemble) with the Berendsen thermal coupling method (49).

In the production procedure, the NVT canonical ensemble was performed with 0.4 ps of temperature coupling decay time for the Berendsen thermal coupling method for 20 ns (50). The MD trajectory was analyzed using Analyze Trajectory module in DS 2.5. The SHAKE algorithm was performed to fix the hydrogen atoms.

Docking

Table I shows the ranking of nine TCM candidates and the control, 3-methylthymidine, based on their Dock Scores. The top two compounds, (*S*)-tryptophan-betaxanthin, and 3-methoxytyramine-betaxanthin obtained significantly higher Dock Scores than the other candidates, suggesting high initial binding affinities. Nevertheless, all candidates demonstrated much higher Dock Score than 3-methylthymidine, which scored 47.18. The piecewise linear potential (PLP) scores gave more detailed information of hydrogen bond (H-bond) contributions to the binding (50). (*S*)-Tryptophan-betaxanthin, 3-methoxytyramine-betaxanthin, gallic acid, and 3-methylthymidine showed higher contributions of H-bond to the binding affinities. Additionally, higher potential mean force (PMF) values (51) on these compounds further supported protein-ligand compatibility. As shown in Figure 1, the candidates were docked into the cavity enclosed by beta sheets, where the surroundings were

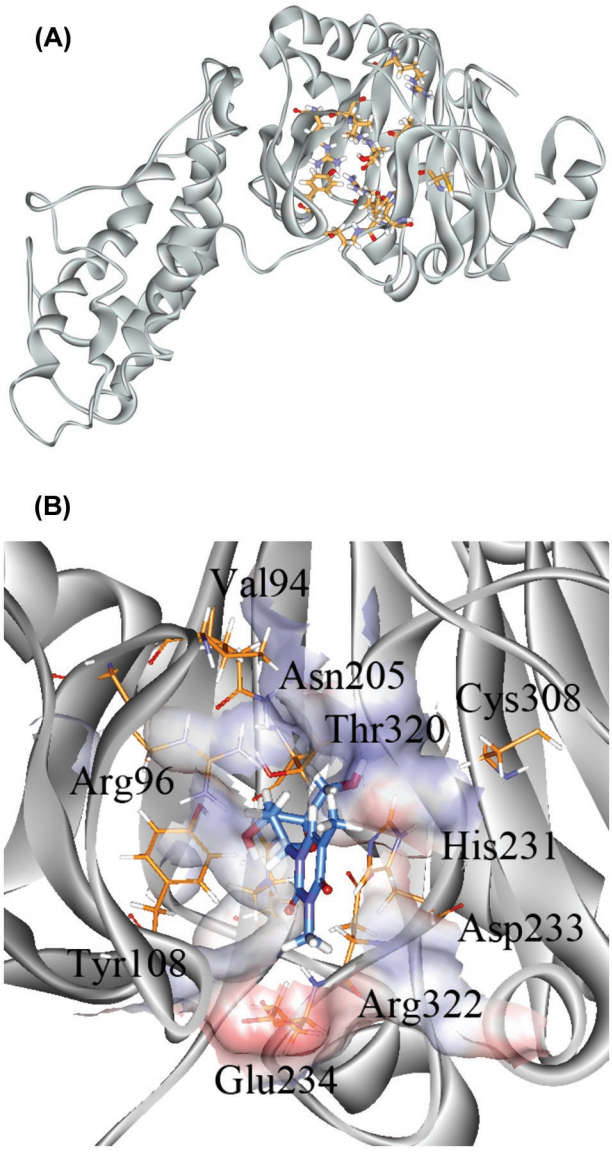

Figure 1: 3D structure of FTO protein and its binding site. (**A**) Whole FTO protein where the ligand binding site was surrounded by the residues in stick style. (**B**) Closeup view of the binding site with an attached ligand (Lapatinib).

predominately polar residues (Figure 1(B)). Based on the 2D structural information (Figure 2), (*S*)-tryptophan-betaxanthin and 3-methoxytyramine-betaxanthin shared structural similarities at the tetrahydropyridine-2,6-dicarboxylate region as well as the ethylidene linker to a second ring structure. The other candidates, except canavanine, are molecules centralized with a single phenyl structure, which were structurally more related to 3-methylthymidine (Figure 2).

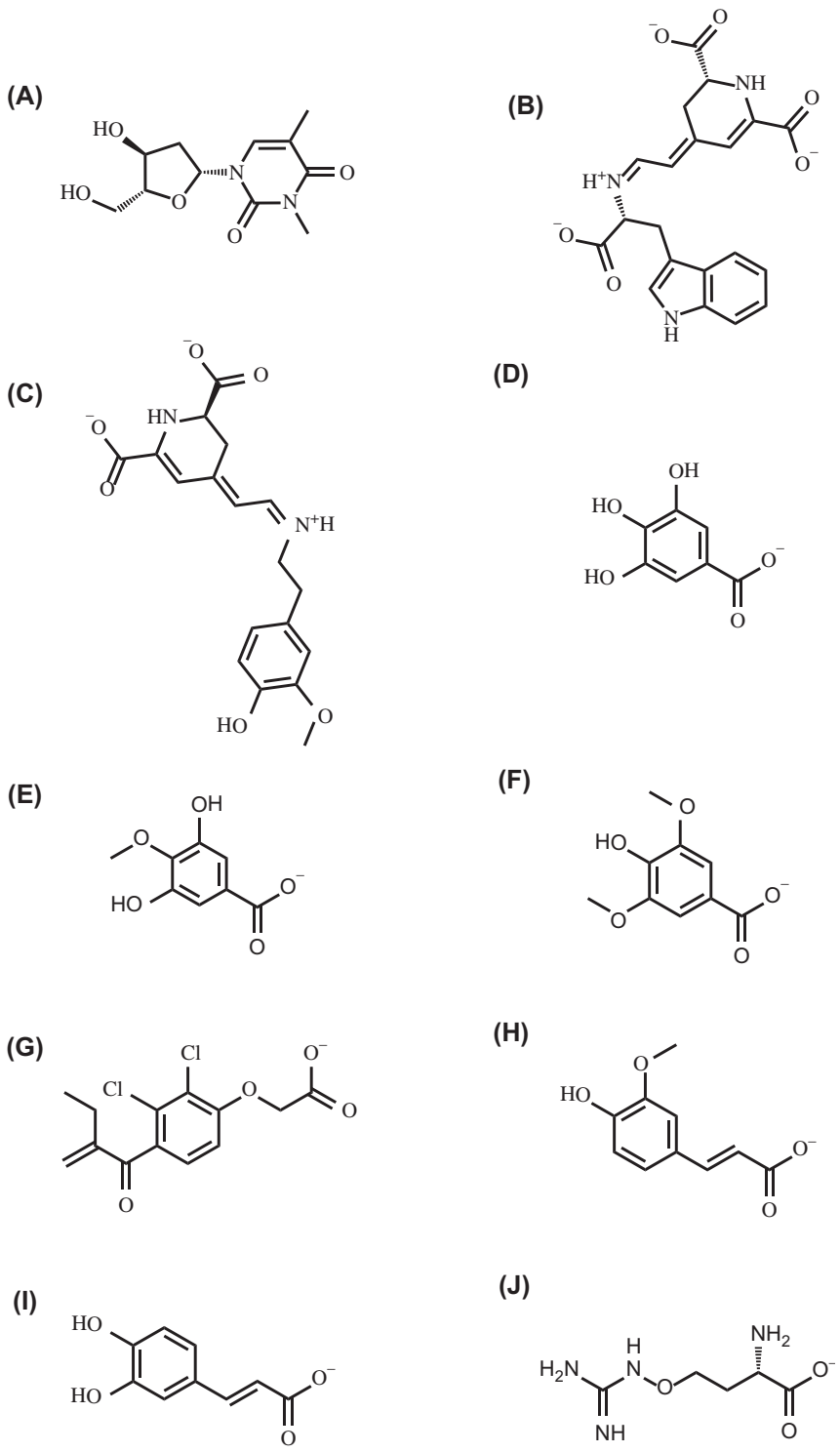

Figure 2: 2D-scaffold structures of (**A**) 3-Methylthymidine (control), and top nine TCM candidates, (**B**) (*S*)-Tryptophan-Betaxanthin, (**C**) 3-Methoxytyramine- Betaxanthin, (**D**) Gallic Acid, (**E**) 4-O-methylgallic Acid, (**F**) Syringic Acid, (**G**) Ethacrynic Acid, (**H**) Ferulic Acid, (**I**) Caffeic Acid, and (**J**) Canavanine.

The docking poses of the top three candidates and 3-methylthymidine were further analyzed (Figure 3). Based on the docking pose of 3-methylthymidine, the H-bond to Arg96 and the pi-pi interaction with His231 were suggested as critical interactions for binding affinities (Figure 3(A)). H-bonds mediated by Arg96 were also observed in the top three ligands. Comparatively, His231 showed slightly weaker pi-mediated interactions in the docking poses. For (*S*)-tryptophan-betaxanthin, the nitrogen on the linker region had weak pi-cation interaction with His231 at a distance of 6.7 Å, which was not captured by the 6.0 Å cutoff (52). Additional H-bonds between FTO and (*S*)-tryptophan-betaxanthin were seen at Asp233, Arg322, and Tyr108, which were associated with the carboxyl groups on the ligand. 3-methoxytyramine-betaxanthin showed stronger pi-cation interaction with His231 at the initial docking pose (Figure 3(C)). Similar to (*S*)-tryptophan-betaxanthin, 3-methoxytyramine-betaxanthin formed a number of H-bonds with between ligand carboxyl groups and residues Arg322, Asn205, and Arg316. Additionally, 3-methoxytyramine-betaxanthin also formed H-bonds with Ala227 and Ser229. Gallic acid has distinct binding poses due to structural differences from other ligands (Figure 3(D)). Intriguingly, Arg96 played a more significant role pi-cation interactions. Residue Arg322 formed an H-bond with the carboxyl group on gallic acid. All candidates demonstrated higher numbers of intermolecular interactions than 3-methylthymidine, which suggest their potencies in competitive inhibition of FTO. MD simulation was then conducted to analyze the dynamic binding stabilities of each candidate.

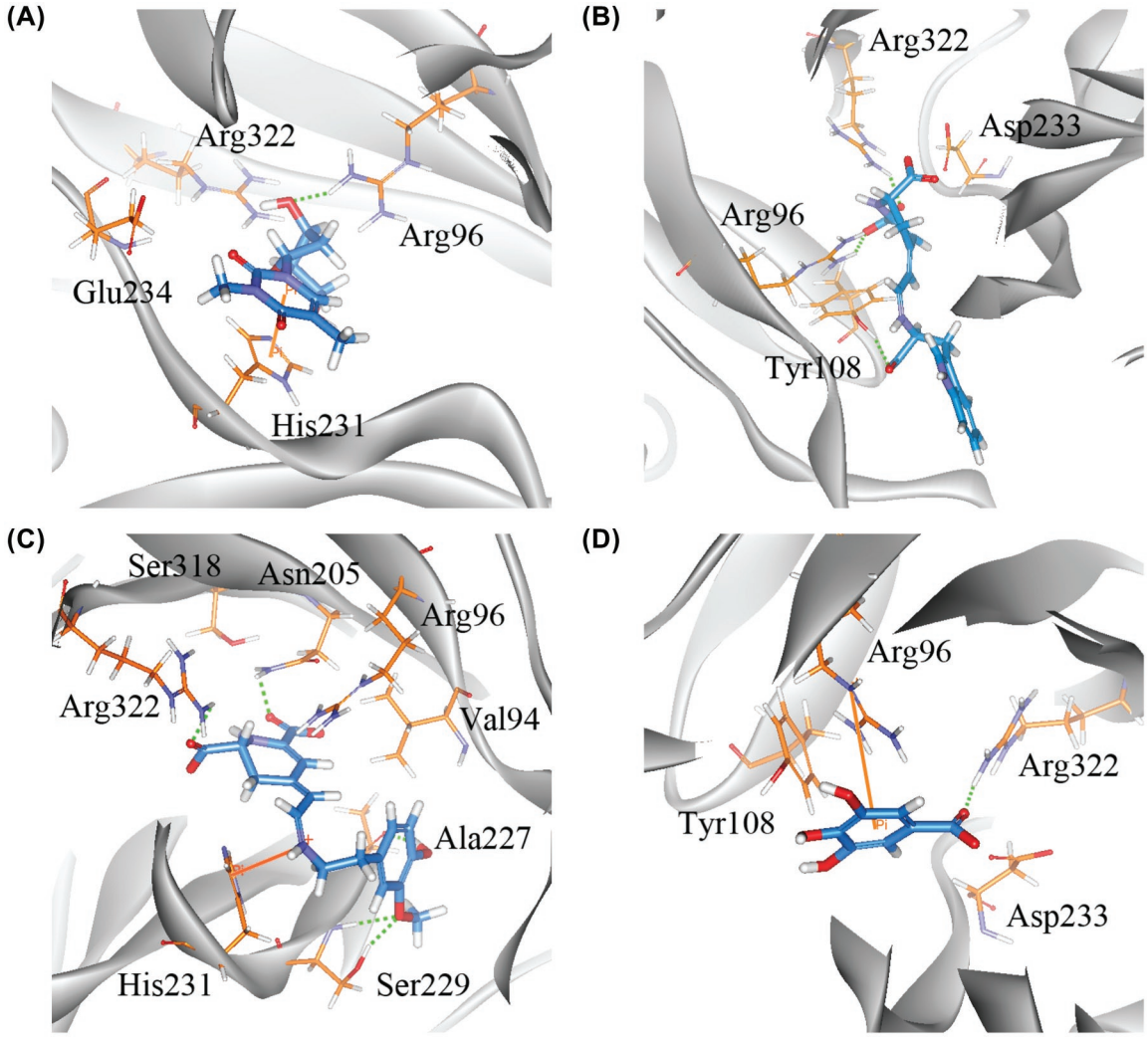

Figure 3: The docking poses of (**A**) 3-Methylthymidine, (**B**) (*S*)-Tryptophan-Betaxanthin, (**C**) 3-Methoxytyramine-Betaxanthin, and (**D**) Gallic acid within the FTO binding site. The pi interactions and H-bonds formed with the main peptide chain are represented by orange line and green dash lines, respectively.

A 20 ns MD simulation was performed for 3-methylthymidine and the top three candidates. Root mean square deviation (RMSD) was measured to assess the magnitude of position displacement before and after simulation. The protein-ligand complex RMSDs (Figure 4(A)) showed stabilizing trends after 6 ns and the RMSDs were maintained at approximately 1.6 Å for all ligands. Based on ligand RMSDs (Figure 4(B)), the top three ligands stabilized after approximately 5 ns of simulation. Intriguingly, 3-methylthymidine showed higher fluctuation rate than the candidates. This could suggest that the three TCM candidates have higher binding stabilities to FTO. Nevertheless, the RMSD fluctuation of the control is limited within 1.2 Å, suggesting moderate binding stability (Figure 4(B)). The total energy trajectories for all ligands also indicate stabilizing trends (Figure 4(C)). Binding stabilities were also suggested by total energy trajectories, in which (*S*)-tryptophan-betaxanthin has the lowest energy state, followed by 3-methoxytyramine-betaxanthin and gallic acid. 3-Methylthymidine has comparatively higher energy states than the candidates, which correspond to the Dock Score rankings shown in Table I.

Considering the significant role an H-bond plays in molecular docking, we tracked the H-bond occupancies for all complexes with a 2.5 Å cutoff during MD (Table II). 3-Methylthymidine formed a total of Eight H-bonds, in which the H-bonds formed with Arg322 and Cys308 were most stable with 49.90% and 44.20% occupancies, respectively. These two H-bonds were stabilized at the end of the simulation. The H-bonds with Arg96 showed more fluctuation, but the relative poses were maintained (Figure 5). Although H-bonds formed at His231, Asp233, Glu234 and Thr320 with 3-methylthymidine have low occupancies according to Table II, these H-bonds were mostly formed (with cutoff of 3 Å) near the end of the simulation (Figure 5).

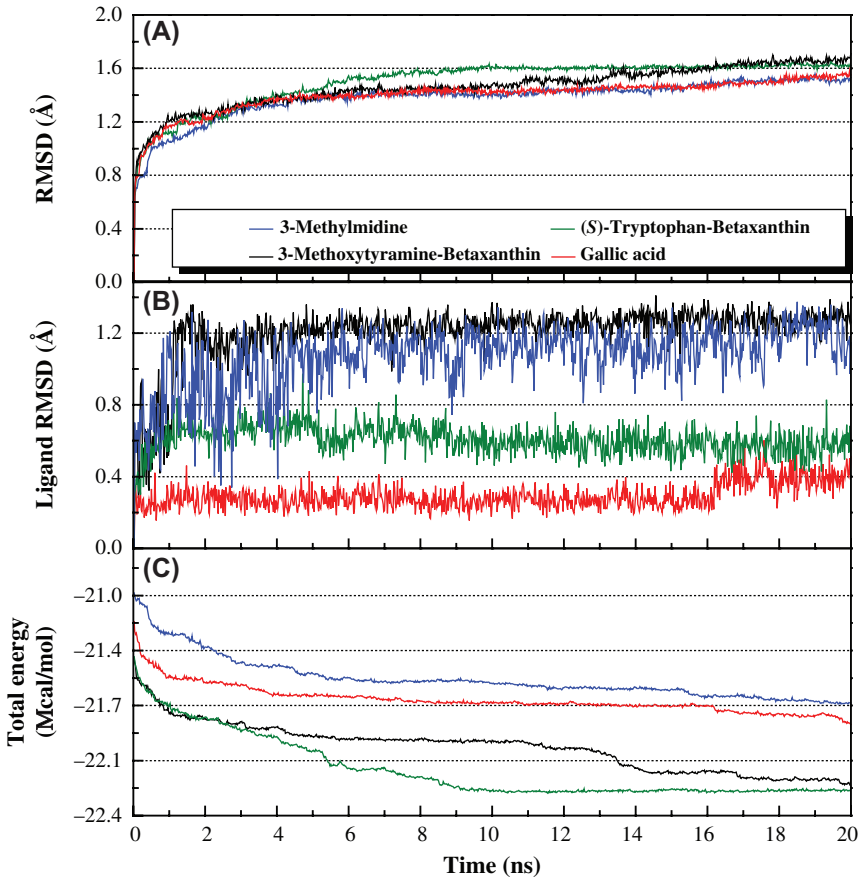

Figure 4: Trajectories of (**A**) Complex RMSD, (**B**) Ligand RMSD, and (**C**) Total energy over the 20 ns MD simulation.

Over the 20 ns simulation, (*S*)-tryptophan-betaxanthin formed four stable H-bonds of over 95% occupancies at 2.5 Å cutoff, which suggested that Arg322 (three bonds) and Ala227 (one bond) were the predominant residues contributing to ligand stability (Table II). With 3.0 Å cutoffs, most of the weaker H-bonds were revealed as participants for protein-ligand stabilization (Figure 6). Intriguingly, the H-bond mediated through Tyr108 at initial docking was broken at the beginning of the simulation, suggesting a possible alternation in binding poses. Nevertheless, the broken H-bond was brought back to approximately 3 Å after 0.5 ns of simulation.

Table I

Docking results of top nine TCM compounds and the control 3-methylthymidine. Data was ranked by Dock Scores.

Name	PLP1	PLP2	PMF	Dock Score
(*S*)-Tryptophan-Betaxanthin	96.31	96.24	158.99	276.12
3-Methoxytyramine-Betaxanthin	84.13	84.26	116.84	247.05
Gallic Acid	57.37	61.80	117.57	106.73
4-O-Methylgallic Acid	12.30	18.21	8.25	106.71
Syringic Acid	56.08	54.61	111.54	106.39
Ethacrynic Acid	25.07	32.66	42.17	106.27
Ferulic Acid	17.22	21.25	14.88	106.01
Caffeic Acid	14.97	19.41	13.32	105.59
Canavanine	49.99	49.91	101.37	104.80
3-Methylthymidine*	69.56	58.21	119.41	47.18

*Control.

Comparatively, high-occupancy (>95%) H-bonds in 3-methoxytyramine-betaxanthin were observed at Asn205, Ala227, His231, and Arg316 (Table II). As shown in Figure 7, the H-bond between Arg316 and ligand atom O23 acted as a temporary

Table II

H-bond occupancies of the control and the top three candidates over the 20 ns MD simulation.

Ligand	H-bond	Ligand atom	Amino acid	Max. distance	Min. distance	Average distance	H-bond occupancy
3-Methylthymidine	1	H30	THR320 : OG1	4.20	2.48	3.4	0.10%
	2	H34	CYS308 : O	2.99	1.98	2.51	44.20%
	3	O14	ARG322 : HH22	3.09	1.78	2.48	49.90%
	4	O14	ARG96 : HH21	3.77	2.09	2.82	18.80%
	5	O14	ARG96 : HH22	3.62	2.07	2.76	22.60%
	6	O3	GLU234 : HN	3.78	2.39	2.95	1.80%
	7	H34	HIS231 : NE2	3.95	2.49	3.18	0.10%
	8	H30	ASP233 : OD2	5.01	1.87	3.26	9.60%
(*S*)-Tryptophan-Betaxanthin	1	H34	ALA227 : O	3.08	1.8	2.2	94.00%
	2	O28	ARG322 : HE	2.67	1.77	2.11	99.20%
	3	O28	ARG322 : HH21	2.76	1.82	2.21	98.40%
	4	O29	ARG322 : HH21	2.48	1.66	1.94	99.90%
	5	O25	ASN205 : HD22	3.56	2.19	2.85	5.80%
	6	O22	VAL94 : HN	3.63	2.44	3.02	0.30%
	7	O23	TYR108 : HH	3.81	2.24	2.86	2.20%
	8	O25	ASN205 : HD21	4.49	2.34	3.31	0.30%
3-Methoxytyramine-Betaxanthin	1	H29	HIS231 : NE2	2.74	1.9	2.22	96.00%
	2	H42	ALA227 : O	2.79	1.74	2.16	97.20%
	3	O22	ARG316 : HH21	3.17	2.25	2.67	10.40%
	4	O23	ARG316 : HH21	3.95	1.71	2.83	19.90%
	5	O22	ARG316 : HH22	2.87	1.78	2.2	94.50%
	6	O22	ASN205 : HD22	2.54	1.73	2.02	99.70%
	7	O23	ASN205 : HD22	4.05	1.94	2.56	50.40%
	8	O19	VAL94 : HN	3.95	2.46	3.16	0.10%
	9	O23	ARG96 : HH21	5.16	2.18	3.41	1.70%
Gallic Acid	1	H16	TYR108 : OH	2.61	1.81	2.14	99.50%
	2	H17	TYR108 : OH	3.30	2.02	2.68	20.00%
	3	O8	TYR108 : HH	3.33	2.29	2.85	1.20%
	4	O9	TYR108 : HH	2.46	1.58	1.92	99.90%

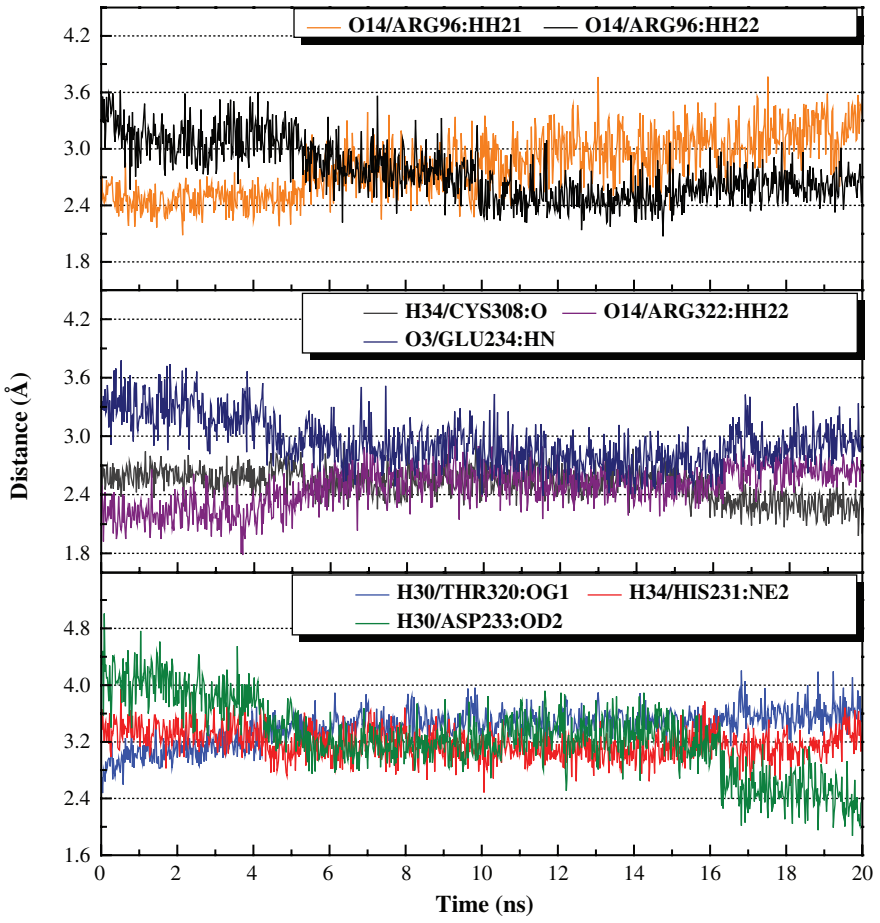

Figure 5: H-bond distance trajectories of 3-methylthymidine in FTO protein during 20 ns MD simulation.

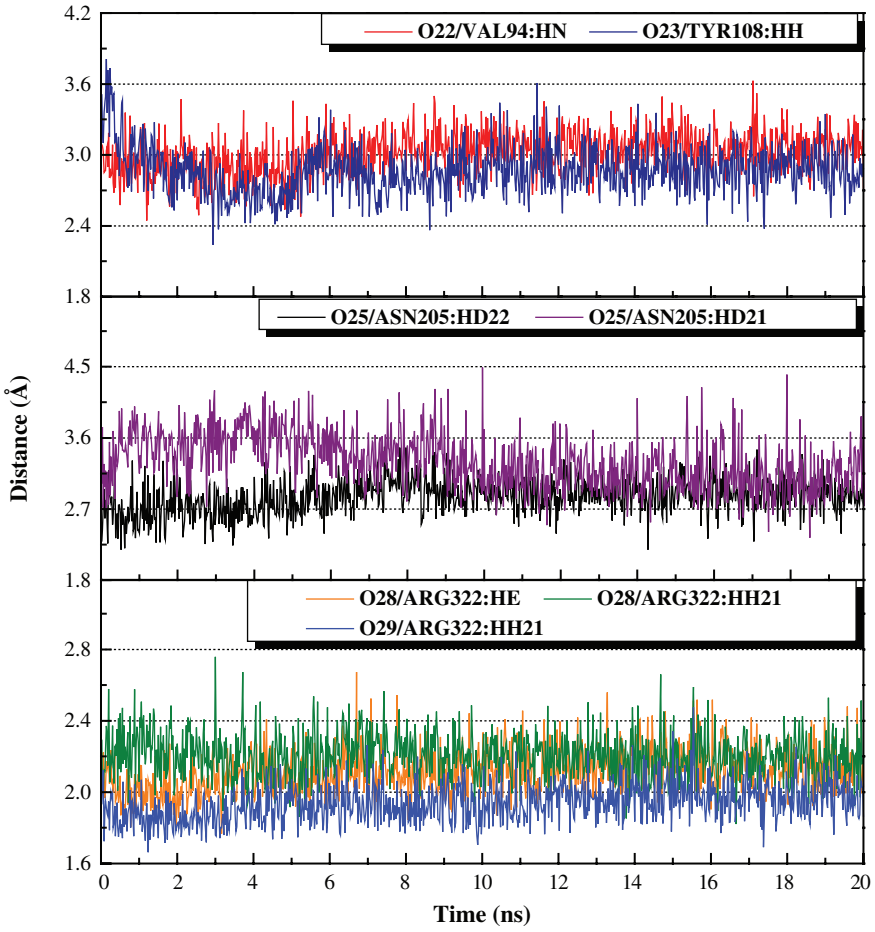

Figure 6: H-bond distance trajectories of (*S*)-tryptophan-betaxanthin in FTO protein during 20 ns MD simulation.

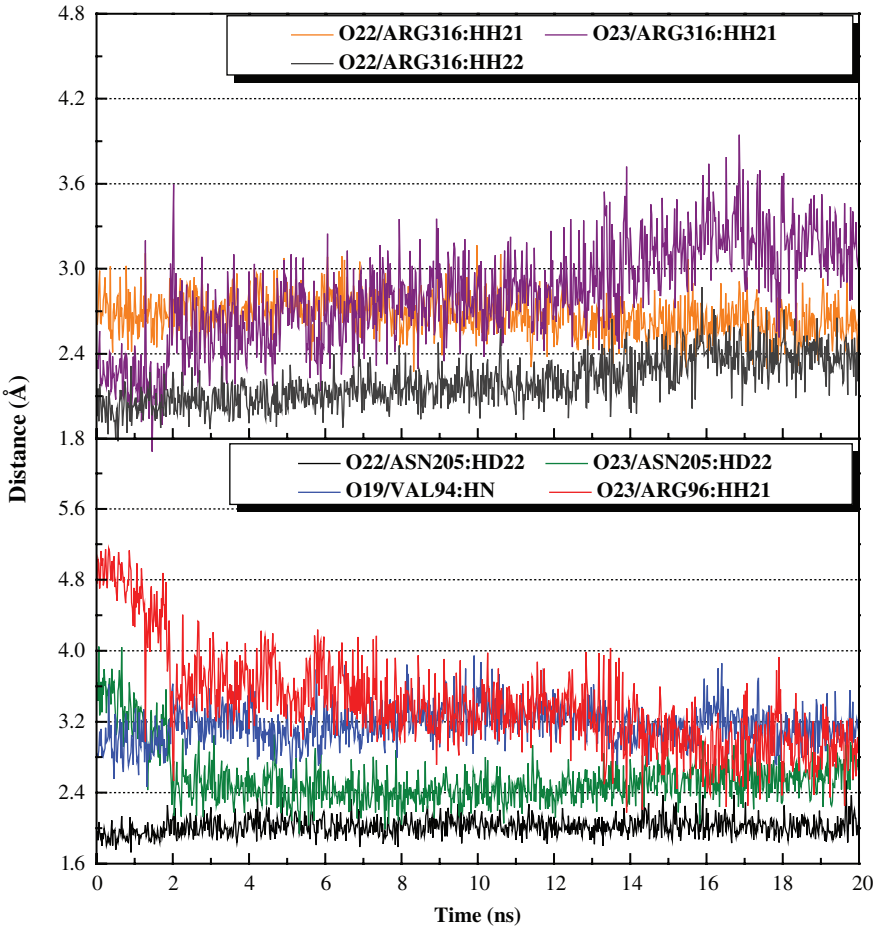

Figure 7: H-bond distance trajectories of 3-methoxytyramine-betaxanthin in FTO protein during 20 ns MD simulation.

ligand binder which the binding distance lengthened over time during the simulation. Intriguingly, O23 formed H-bonds with Arg96 and Asn205 after approximately 2 ns (Figure 7). The distinct changes associated with O23-linked H-bond distance trajectories suggested alteration in ligand pose. This change could also account for the fluctuation in ligand RMSD at 2 ns simulation (Figure 4(B)).

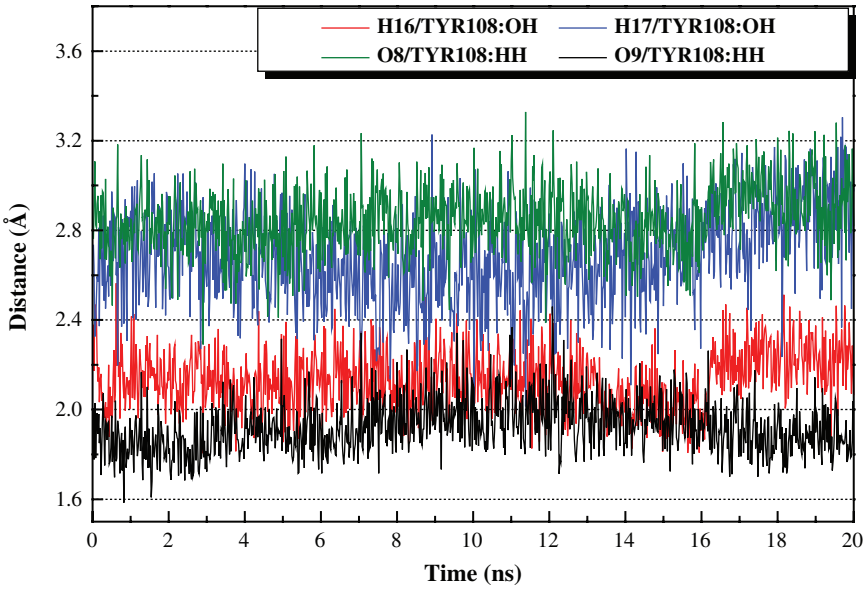

Figure 8: H-bond distance trajectories of gallic acid in FTO protein during 20 ns MD simulation.

Gallic acid is comparatively smaller than (*S*)-tryptophan-betaxanthin and 3-methoxytyramine-betaxanthin. Only two H-bonds were observed for gallic acid during the simulation (Table II). However, the two H-bond occupancies of over 99.00% between ligand and Tyr108 suggested the interactions had strong binding affinities, despite high deviation in bond distances (Figure 8).

Based on the H-bond distance trajectories, we further compared non-stabilized docking pose with the stabilized pose for each TCM candidates. Figure 9(A) and 9(B) show the docking pose of 3-methylthymidine before and after stabilization. Two additional H-bonds with Asp233 and Glu234 were observed. 3-Methylthymidine

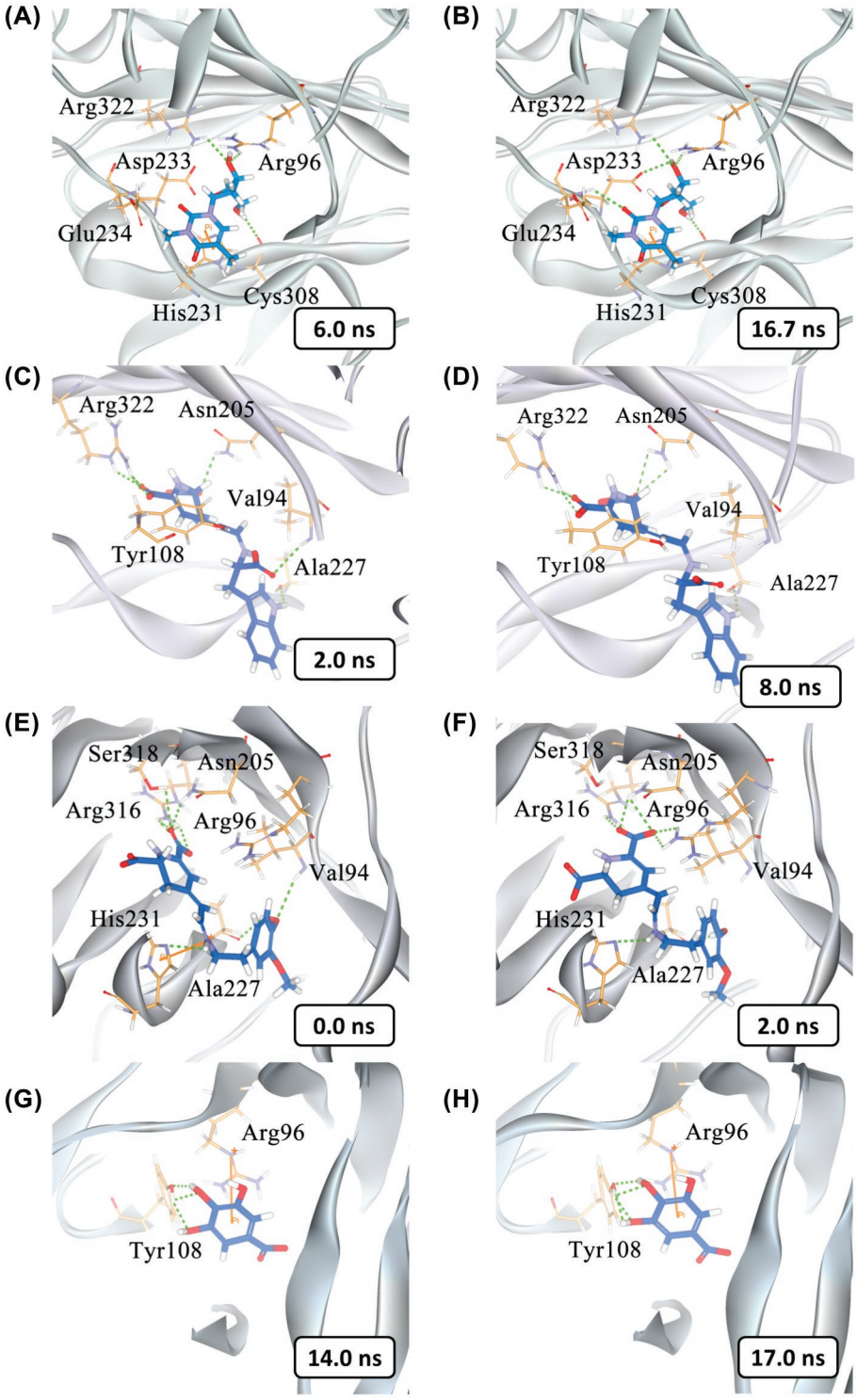

Figure 9: MD simulation snapshots of 3-methylthymidine (**A, B**), (*S*)-tryptophan-betaxanthin (**C, D**), 3-methoxytyramine-betaxanthin (**E, F**), and gallic acid (**G, H**).

was pulled closer toward His231 by pi-pi interaction and the additional H-bonds (Figure 9(B), Video S1). For (*S*)-tryptophan-betaxanthin (Figure 9(C) and 9(D)), the H-bonds with Arg322 were maintained throughout the simulation. Moreover, the two H-bonds with Asn205 shifted to a more stable state in which the interaction lengths became similar (Video S2). These interactions were believed to hinder the natural ligands, 3-methylthymidine or 3-methyluracil (53), from docking onto FTO. With regard to 3-Methoxytyramine-betaxanthin, the tetrahydropyridine ring rotated during the first two nanoseconds. This rotation brought one of its carboxylates closer to the binding residues. Subsequently, additional H-bonds with Asn205 and Arg96 were formed (Figure 9(E), 9(F)). Although the conformation change broke the pi-cation interaction with His231, the newly formed H-bonds were able to maintain the ligand within the binding site, in particular with the key residue Arg96 (Video S3). Comparatively, gallic acid was a less stable compound which had high H-bond distance fluctuations. Nevertheless, its binding pose was maintained by the pi-cation interaction with Arg96. The H-bonds with Tyr108 at 17 ns further restricted the ligand within a pre-defined region (Figure 9(G), 9(H), Video S4).

Formation of H-bonds at Arg96 and Glu234 are critical to substrate specificity of the FTO protein (46). The formation of either H-bond or pi-interaction with Arg96 was also observed for the TCM candidates (Figure 9). Though interactions with Glu234 were not detected in the TCM candidates, other H-bonds formed with the binding site contribute to stable ligand-protein complexes and the binding of other ligands within the binding site is unlikely. By blocking Arg96, which is critical to FTO activity, the TCM candidates show good potential as FTO inhibitors.

Based on the MD simulation, both (*S*)-tryptophan-betaxanthin and 3-methoxytyramine-betaxanthin have sufficient H-bonds to maintain binding stabilities. 3-Methylthymidine also formed a number of H-bonds that stabilized the protein-ligand binding poses. Gallic acid was maintained in the FTO docking site in a more dynamic fashion. Nevertheless, all top three ligands are candidates that may competitively inhibit FTO functions.

Conclusion

We analyzed both binding affinities and binding stabilities of potential FTO inhibitors from TCM Database@Taiwan (44) using structure-based virtual screening and MD simulation. All top three ligands obtained higher Dock Scores than the control. During MD, both (*S*)-tryptophan-betaxanthin and 3-methoxytyramine-betaxanthin formed a number of additional H-bonds that might strengthen the protein-ligand binding affinities. Gallic acid did not form additional H-bonds, but existing H-bonds and the pi-cation interaction held the ligand at a fixed position. Based on the *in silico* analysis, all three candidates were suggested as potential competitive FTO inhibitors that hinder the protein's demethylation functions.

Supplementary Material

Supplementary materials consist of videos of the interaction between FTO and the various potential candidates. Also shown are the snapshots of docking and re-docking at the FTO binding site. They appear at the JBSD website where the article appears.

Acknowledgements

The research was supported by grants from the National Science Council of Taiwan (NSC 99-2221-E-039-013-), Committee on Chinese Medicine and Pharmacy (CCMP100-RD-030), China Medical University, China Medical University Beigang Hospital and Asia University (CMU98-TCM, CMU99-TCM, CMU99-S-02,

CMU99-ASIA-25, CMU99-ASIA-26 CMU99-ASIA-27 CMU99-ASIA-28 CMUBHR100-012). This study is also supported in part by Taiwan Department of Health Clinical Trial and Research Center of Excellence (DOH100-TD-B-111-004) and Taiwan Department of Health Cancer Research Center of Excellence (DOH100-TD-C-111-005). We are grateful to the Asia University cloud-computing facilities.

References

1. T. M. Frayling, N. J. Timpson, M. N. Weedon, E. Zeggini, R. M. Freathy, C. M. Lindgren, J. R. B. Perry, K. S. Elliott, H. Lango, N. W. Rayner, B. Shields, L. W. Harries, J. C. Barrett, S. Ellard, C. J. Groves, B. Knight, A. M. Patch, A. R. Ness, S. Ebrahim, D. A. Lawlor, S. M. Ring, Y. Ben-Shlomo, M. R. Jarvelin, U. Sovio, A. J. Bennett, D. Melzer, L. Ferrucci, R. J. F. Loos, I. Barroso, N. J. Wareham, F. Karpe, K. R. Owen, L. R. Cardon, M. Walker, G. A. Hitman, C. N. A. Palmer, A. S. F. Doney, A. D. Morris, G. D. Smith, A. T. Hattersley, M. I. McCarthy, and W. T. C. Control. *Science 316*, 889-894 (2007).
2. L. Qi, K. Kang, C. Zhang, R. M. van Dam, P. Kraft, D. Hunter, C. H. Lee, and F. B. Hu. *Diabetes 57*, 3145-3151 (2008).
3. N. J. Poritsanos, P. S. Lew, and T. M. Mizuno. *Biochem Biophys Res Commun 400*, 713-717 (2010).
4. C. Church, L. Moir, F. McMurray, C. Girard, G. T. Banks, L. Teboul, S. Wells, J. C. Bruning, P. M. Nolan, F. M. Ashcroft, and R. D. Cox. *Nat Genet 42*, 1086-1092 (2010).
5. D. Tews, P. Fischer-Posovszky, and M. Wabitsch. *Horm Metab Res 43*, 17-21 (2011).
6. G. Stratigopoulos and R. L. Leibel. *Nat Genet 42*, 1038-1039 (2010).
7. Z. Pausova, C. Syme, M. Abrahamowicz, Y. Xiao, G. T. Leonard, M. Perron, L. Richer, S. Veillette, G. D. Smith, O. Seda, J. Tremblay, P. Hamet, D. Gaudet, and T. Paus. *Circ Cardiovasc Genet 2*, 260-269 (2009).
8. K. Hotta, T. Kitamoto, A. Kitamoto, S. Mizusawa, T. Matsuo, Y. Nakata, S. Kamohara, N. Miyatake, K. Kotani, R. Komatsu, N. Itoh, I. Mineo, J. Wada, M. Yoneda, A. Nakajima, T. Eunahashi, S. Miyazaki, K. Tokunaga, H. Masuzaki, T. Ueno, K. Hamaguchi, K. Tanaka, K. Yamada, T. Hanafusa, S. Oikawa, H. Yoshimatsu, T. Sakata, Y. Matsuzawa, K. Nakao, and A. Sekine. *J Hum Genet 56*, 647-651 (2011).
9. N. J. Timpson, R. Harbord, G. Davey Smith, J. Zacho, A. Tybiaerg-Hansen, B. G. Nordestgaard. *Hypertension 54*, 84-90 (2009).
10. Q. Yan, J. Hong, W. Gu, Y. Zhang, Q. Liu, Y. Su, X. Li, B. Cui, and G. Ning. *Endocrine 36*, 377-382 (2009).
11. E. Wehr, N. Schweighofer, R. Moller, A. Giuliani, T. R. Pieber, and B. Obermayer-Pietsch. *Metab-Clin Exp 59*, 575-580 (2010).
12. L. Keller, W. L. Xu, H. X. Wang, B. Winblad, L. Fratiglioni, and C. Graff. *J Alzheimers Dis 23*, 461-469 (2011).
13. V. Kaklamani, N. Yi, M. Sadim, K. Siziopikou, K. Zhang, Y. Xu, S. Tofilon, S. Agarwal, B. Pasche, and C. Mantzoros. *BMC Medical Genetics 12*, 52 (2011).
14. A. J. Ho, J. L. Stein, X. Hua, S. Lee, D. P. Hibar, A. D. Leow, I. D. Dinov, A. W. Toga, A. J. Saykin, L. Shen, T. Foroud, N. Pankratz, M. J. Huentelman, D. W. Craig, J. D. Gerber, A. N. Allen, J. J. Corneveaux, D. A. Stephan, C. S. DeCarli, B. M. DeChairo, S. G. Potkin, C. R. Jack Jr., M. W. Weiner, C. A. Raji, O. L. Lopez, J. T. Becker, O. T. Carmichael, P. M. Thompson, and the Alzheimer's Disease Neuroimaging Initiative. *Proc Natl Acad Sci U S A 107*, 8404-8409 (2010).
15. J. A. Benedict, E. Jacobsson, E. Ronnemaa, M. Saliman-Almen, S. Brooks, B. Schultes, R. Fredriksson, L. Lannfelt, L. Kilander, H. B. Schloth. *Neurobiol Aging 32*, 1159 e1-5 (2011).
16. K. G. Ewens, M. R. Jones, W. Ankener, D. R. Stewart, M. Urbanek, A. Dunaif, R. S. Legro, A. Chua, R. Azziz, R. S. Spielman, M. O. Goodarzi, and J. F. Strauss III. *PLoS ONE 6*, e16390 (2011).
17. T. Gerken, C. A. Girard, Y. C. L. Tung, C. J. Webby, V. Saudek, K. S. Hewitson, G. S. H. Yeo, M. A. McDonough, S. Cunliffe, L. A. McNeill, J. Galvanovskis, P. Rorsman, P. Robins, X. Prieur, A. P. Coll, M. Ma, Z. Jovanovic, I. S. Farooqi, B. Sedgwick, I. Barroso, T. Lindahl, C. P. Ponting, F. M. Ashcroft, S. O'Rahilly, and C. J. Schofield. *Science 318*, 1469-1472 (2007).
18. P. K. Olszewski, K. J. Radomska, K. Ghimire, A. Klockars, C. Ingman, A. M. Olszewska, R. Fredriksson, A. S. Levine, and H. B. Schioth. *Physiol Behav 103*, 248-253 (2011).
19. Y.-C. L. Tung, E. Ayuso, X. Shan, F. Bosch, S. O'Rahilly, A. P. Coll, and G. S. H. Yeo. *PLoS ONE 5*, e8771 (2009).
20. C. Q. Yi, G. F. Jia, G. H. Hou, Q. Dai, W. Zhang, G. Q. Zheng, X. Jian, C. G. Yang, Q. A. Cui, and C. A. He. *Nature 468*, 330-333 (2010).
21. C. Zabena, J. L. Gonzalez-Sanchez, M. T. Martinez-Larrad, A. Torres-Garcia, J. Alvarez-Fernandez-Represa, A. Corbaton-Anchuelo, M. Perez-Barba, and M. Serrano-Rios. *Obes Surg 19*, 87-95 (2009).

22. A. Hinney, T. T. Nguyen, A. Scherag, S. Friedel, G. Brönner, T. D. Muller, H. Grallert, T. Illig, H. E. Wichmann, W. Rief, H. Schafer, and J. Hebebrand. *PLoS ONE 2*, e1361 (2007).
23. K. Wang, W.-D. Li, C. K. Zhang, Z. Wang, J. T. Glessner, S. F. Grant, H. Zhao, H. Hakonarson, and R. A. Price. *PLoS ONE 6*, e18939 (2011).
24. I. S. Farooq. *Cell Metabolism 13*, 7-8 (2011).
25. *World Health Organization, Obesity and overweight, Fact sheet N°311* (2011).
26. M. D. Yang, K. C. Lai, T. Y. Lai, S. C. Hsu, C. L. Kuo, C. S. Yu, M. L. Lin, J. S. Yang, H. M. Kuo, S. H. Wu, and J. G. Chung. *Anticancer Res 30*, 2135-2143 (2010).
27. J. Fischer, L. Koch, C. Emmerling, J. Vierkotten, T. Peters, J. C. Bruning, and U. Ruther. *Nature 458*, 894-898 (2009).
28. T. Ahmad, D. I. Chasman, S. Mora, G. Pare, N. R. Cook, J. E. Buring, P. M. Ridker, and I. M. Lee. *Am Heart J 160*, 1163-1169 (2010).
29. P. P. Wu, K. C. Liu, W. W. Huang, C. Y. Ma, H. Lin, J. S. Yang, and J. G. Chung. *Oncol Rep 25*, 551-557 (2011).
30. Y. M. Leung, Y. H. Tsou, C. S. Kuo, S. Y. Lin, P. Y. Wu, M. J. Hour, and Y. H. Kuo. *Phytomedicine 18*, 46-51 (2010).
31. H. Brotz-Oesterhelt, D. Beyer, H. P. Kroll, R. Endermann, C. Ladel, W. Schroeder, B. Hinzen, S. Raddatz, H. Paulsen, K. Henninger, J. E. Bandow, H. G. Sahl, and H. Labischinski. *Nat Med 11*, 1082-1087 (2005).
32. K.-C. Chen and C. Y.-C. Chen. *Soft Matter 7*, 4001-4008 (2011).
33. M. Rottmann, C. McNamara, B. K. Yeung, M. C. Lee, B. Zou, B. Russell, P. Seitz, D. M. Plouffe, N. V. Dharia, J. Tan, S. B. Cohen, K. R. Spencer, G. E. Gonzalez-Paez, S. B. Lakshminarayana, A. Goh, R. Suwanarusk, T. Jegla, E. K. Schmitt, H. P. Beck, R. Brun, F. Nosten, L. Renia, V. Dartois, T. H. Keller, D. A. Fidock, E. A. Winzeler, and T. T. Diagana. *Science 329*, 1175-1180 (2010).
34. P. Filippakopoulos, J. Qi, S. Picaud, Y. Shen, W. B. Smith, O. Fedorov, E. M. Morse, T. Keates, T. T. Hickman, I. Felletar, M. Philpott, S. Munro, M. R. McKeown, Y. Wang, A. L. Christie, N. West, M. J. Cameron, B. Schwartz, T. D. Heightman, N. La Thangue, C. A. French, O. Wiest, A. L. Kung, S. Knapp, and J. E. Bradner. *Nature 468*, 1067-1073 (2010).
35. K. Dhanachandra Singh, M. Karthikeyan, P. Kirubakaran, and S. Nagamani. *J Mol Graph Model 30*, 186-197 (2011).
36. T. Knehans, A. Schuller, D. N. Doan, K. Nacro, J. Hill, P. Guntert, M. S. Madhusudhan, T. Weil, and S. G. Vasudevan. *J Comput Aided Mol Des 25*, 263-274 (2011).
37. P. Fedichev, R. Timakhov, T. Pyrkov, E. Getmantsev, and A. Vinnik. *PLoS Curr 3*, RRN1253 (2011).
38. R. V. Guido, G. Oliva, and A. D. Andricopulo. *Curr Med Chem 15*, 37-46 (2008).
39. S. John, S. Thangapandian, S. Sakkiah, and K. W. Lee. *BMC Bioinformatics 12*, *Suppl 1*, S28 (2011).
40. C. Y. Chen and C. Y. C. Chen. *J Mol Graph Model 29*, 21-31 (2010).
41. V. Kenyon, G. Rai, A. Jadhav, L. Schultz, M. Armstrong, J. B. Jameson, 2nd, S. Perry, N. Joshi, J. M. Bougie, W. Leister, D. A. Taylor-Fishwick, J. L. Nadler, M. Holinstat, A. Simeonov, D. J. Maloney, and T. R. Holman. *J Med Chem 54*, 5485-5497 (2011).
42. C. Y. C. Chen. *J Mol Graph Model 28,* 261-269 (2009).
43. S. Vilar, G. Ferino, S. S. Phatak, B. Berk, C. N. Cavasotto, and S. Costanzi. *J Mol Graph Model 29,* 614-623 (2011).
44. C. Y. C. Chen. *PLoS One 6*, e15939 (2011).
45. C. A. Lipinski, F. Lombardo, B. W. Dominy, and P. J. Feeney. *Advanced Drug Delivery Reviews 46*, 3-26 (2001).
46. Z. Han, T. Niu, J. Chang, X. Lei, M. Zhao, Q. Wang, W. Cheng, J. Wang, Y. Feng, and J. Chai. *Nature 464*, 1205-1209 (2010).
47. B. R. Brooks, R. E. Bruccoleri, B. D. Olafson, D. J. States, S. Swaminathan, and M. Karplus. *J Comp Chem 4,* 187-217 (1983).
48. C. M. Venkatachalam, X. Jiang, T. Oldfield, and M. Waldman. *J Mol Graph Model 21*, 289-307 (2003).
49. H. J. C. Berendsen, J. P. M. Postma, W. F. van Gunsteren, A. Dinola, and J. R. Haak. *The Journal of Chemical Physics 81*, 3684-3690 (1984).
50. D. K. Gehlhaar, D. Bouzida, and P. A. Rejto. L. Parrill and M. Rami Reddy (Eds.), *American Chemical Society 719*, Washington, DC, 292-311 (1999).
51. I. Muegge and Y. C. Martin. *J Med Chem 42*, 791-804 (1999).
52. D. A. Dougherty. *Science 271*, 163-168 (1996).
53. G. Jia, C. G. Yang, S. Yang, X. Jian, C. Yi, Z. Zhou, and C. He. *FEBS Lett 582*, 3313-3319 (2008).

Date Received: May 11, 2011

Communicated by the Editor Ramaswamy H. Sarma